Pharm Res (2014) 31:449–465
DOI 10.1007/s11095-013-1174-5

RESEARCH PAPER

Use of a Fundamental Approach to Spray-Drying Formulation Design to Facilitate the Development of Multi-Component Dry Powder Aerosols for Respiratory Drug Delivery

Susan Hoe • James W. Ivey • Mohammed A. Boraey • Abouzar Shamsaddini-Shahrbabak • Emadeddin Javaheri • Sadaf Matinkhoo • Warren H. Finlay • Reinhard Vehring

Received: 22 May 2013 / Accepted: 28 July 2013 / Published online: 23 August 2013

ABSTRACT

Purpose A fundamental approach incorporating current theoretical models into aerosol formulation design potentially reduces experimental work for complex formulations. A D-amino acid mixture containing D-Leucine (D-Leu), D-Methionine, D-Tryptophan, and D-Tyrosine was selected as a model formulation for this approach.

Methods Formulation design targets were set, with the aim of producing a highly dispersible D-amino acid aerosol. Particle formation theory and a spray dryer process model were applied with boundary conditions to the design targets, resulting in *a priori* predictions of particle morphology and necessary spray dryer process parameters. Two formulations containing 60% w/w trehalose, 30% w/w D-Leu, and 10% w/w remaining D-amino acids were manufactured.

Results The design targets were met. The formulations had rugose and hollow particles, caused by deformation of a crystalline D-Leu shell while trehalose remained amorphous, as predicted by particle formation theory. D-Leu acts as a dispersibility enhancer, ensuring that both formulations: 1) delivered over 40% of the loaded dose into the *in vitro* lung region, and 2) achieved desired values of lung airway surface liquid concentrations based on lung deposition simulations.

Conclusions Theoretical models were applied to successfully achieve complex formulations with design challenges *a priori*. No further iterations to the design process were required.

KEY WORDS Antimicrobial · D-amino acids · *in silico* · lung · particle formation model · spray drying

S. Hoe • J. W. Ivey • M. A. Boraey • A. Shamsaddini-Shahrbabak • E. Javaheri • S. Matinkhoo • W. H. Finlay • R. Vehring (✉)
Department of Mechanical Engineering, University of Alberta
Edmonton, Alberta, Canada T6G 2G8
e-mail: reinhard.vehring@ualberta.ca

INTRODUCTION

Spray drying is a well-established technique for the production of pharmaceutical powders. Traditionally, spray drying has been used primarily as a process for reduction of particle size, with less regard given to the other properties of the manufactured powder. However, novel therapeutic approaches to respiratory disease have complex formulation requirements, and as a result there has been an increasing focus on using particle engineering to achieve the desired composition and aerosol performance of these sophisticated formulations (1). This necessitates a solid understanding of particle formation processes in order to achieve required particle and bulk powder attributes (2).

These present-day demands place spray drying as an ideal method for the manufacture of novel, sophisticated aerosol formulations. Spray drying has several adjustable process parameters which have a direct influence on particle formation, including liquid feedstock composition, feed rate, and drying gas temperature. Often, the spray drying process can be adjusted to achieve desired particle properties (3). However, due to the large number of formulation and spray drying process variables, a purely empirical approach to formulation development would be very time-consuming and costly.

Several process models for the spray drying process have been successfully applied (4, 5), which when combined with mechanistic particle formation models (2) assist in the selection of formulation and process parameters for the desired particle and bulk powder properties. With this rational approach to formulation design, one can minimise empirical iterative work, and expedite process and formulation development (6, 7). In this paper, we apply a fundamental approach to the formulation of inhalable powders for *Pseudomonas aeruginosa* biofilm disruption.

Cystic fibrosis presents with mucous airways plugging, leaving the patient highly susceptible to opportunistic respiratory

infections, such as *Pseudomonas aeruginosa* and methicillin-resistant *Staphylococcus aureus* (MRSA) (8), often presenting as a biofilm (Fig. 1), which acts as a unique environment for the diffusion of nutrients and waste to and from the bacteria, conferring antibiotic resistance to mucoid *P. aeruginosa* (9, 10). Antibiotic-resistant strains of *P. aeruginosa* have been reported in CF patient sputum isolates, although the prevalence and temporal trend varies from study to study (11–14). This foreshadows a potential future where CF lung infections are insensitive to antibiotic therapy.

There are emerging options for non-antibiotic antipseudomonal therapy. Kolodkin-Gal *et al.* (15) reported the efficacy of a particular D-amino acid cocktail in disrupting *P. aeruginosa* biofilm growth *in vitro*. An equimolar mixture (5 nM) of D-Leucine (D-Leu), D-Methionine (D-Met), D-Tryptophan (D-Trp) and D-Tyrosine (D-Tyr), was applied to a *P. aeruginosa* PA14 culture and incubated in M63 medium at 30°C for 48 h. Compared against control, and against an equivalent L-amino acid mixture, biofilm growth was effectively prevented (15). Sanchez *et al.* have demonstrated the efficacy of an equimolar D-Leu/D-Met/D-Trp/D-Tyr solution against a flow chamber-grown *P. aeruginosa* biofilm (16). As yet, there have been no published studies testing D-amino acid cocktails against biofilm grown in CF lung lining fluid, so the physiological efficacy of these compounds remains unknown.

The attraction of D-amino acid therapy for respiratory infection lies in its low molecular weight (potentially avoiding issues with diffusivity and penetrating efficiency in biofilms (17)), and the potential to act as adjuvant to existing antimicrobial therapy and other biotherapeutics. Thus, an equimolar quaternary D-amino acid formulation would be an ideal candidate as a spray dried powder delivered to the lungs via aerosol. However, the complexity and novelty of the formulation, as well as the limited aqueous solubility of the D-amino acids, makes process and formulation development challenging.

In this study, we take a fundamental approach to formulation and process design, applying process models and mechanistic particle formation models, to efficiently create dispersible spray dried multi-component D-amino acid formulations for aerosol delivery to the lung. In addition, a lung deposition model was employed to simulate the regional lung deposition and airway surface liquid concentration of the designed aerosol formulation. The following section will summarise the models applied in this study.

Theory

Particle Formation Model

The application of a particle formation model enables prediction of the spatial distribution, crystallinity, and particle morphology for the selected spray dried multi-component formulation. A more extensive explanation of particle formation and drying kinetics is discussed by Vehring *et al* (2).

For a solution droplet containing solutes i with diffusion coefficients D_i and evaporating at evaporation rate κ, the dimensionless Peclet number may be defined as:

$$Pe_i = \frac{\kappa}{8D_i} \tag{1}$$

For small Peclet number (< 1), diffusion is fast relative to droplet evaporation, and the concentration of the component remains uniform in the droplet throughout the evaporation process. When the Peclet number is large, the droplet surface recession is faster than solute diffusion, resulting in high surface enrichment.

The Peclet number can be used to quantify the radial concentration profile in the evaporating droplet. The surface concentration of component i ($c_{s,i}$) relative to the mean droplet concentration for component i ($c_{m,i}$) is expressed as surface enrichment E_i, and may be approximated by an expansion in terms of the Peclet number as

$$E_i = \frac{c_{s,i}}{c_{m,i}} = 1 + \frac{Pe_i}{5} + \frac{Pe_i^2}{100} - \frac{Pe_i^3}{4000} \tag{2}$$

The droplet lifetime (τ_D) is the time taken for a droplet to dry completely:

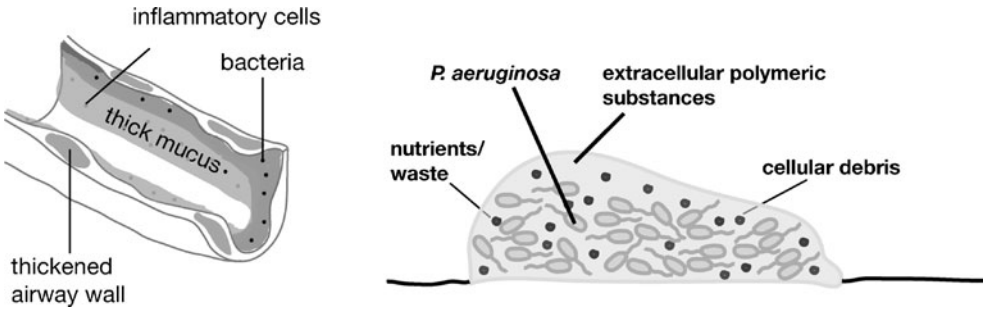

Fig. 1 A cross-section of the airways lumen in the cystic fibrosis lung (*left*), and the typical contents of a bacterial biofilm (*right*).

$$\tau_{\mathrm{D}} = \frac{d_0^2}{\kappa} \tag{3}$$

where d_0 is the initial droplet diameter and κ is the evaporation rate. The saturation time ($\tau_{\mathrm{sat,i}}$), is the time taken for each component i to reach saturation:

$$\tau_{\mathrm{sat,i}} = \tau_{\mathrm{D}}\left[1-\left(\frac{c_{0,\mathrm{i}}E_{\mathrm{i}}}{c_{\mathrm{sol,i}}}\right)^{\frac{2}{3}}\right] \tag{4}$$

where $c_{0,\mathrm{i}}$ is the initial concentration of component *i* in the droplet, and $c_{\mathrm{sol,i}}$ is the solubility of component *i*. Naturally, saturation time is related to solubility and initial concentration; low solubility, or high initial concentration, will reduce $\tau_{\mathrm{sat,i}}$.

After the component reaches saturation, the remaining time between saturation and complete droplet drying is available for crystallisation of the component; this interval is called the precipitation time ($\tau_{\mathrm{p,i}}$) and may be expressed as:

$$\tau_{\mathrm{p,i}} = \tau_{\mathrm{D}}\left[1-\left(\frac{c_{0,i}}{\rho_{\mathrm{t,i}}}\cdot E_{\mathrm{i}}\right)^{\frac{2}{3}}\right] \tag{5}$$

where $\rho_{\mathrm{t,i}}$ is the true density for component *i*. The components which are able to crystallize within the precipitation window, once crystallized, are far less mobile than the solute form, and will experience a significant increase in Peclet number. The consequence is high surface enrichment, and the formation of a crystalline shell with a hollow core. The components which do not have sufficient time to crystallize will remain amorphous in the spray dried particle.

Mass Balance Calculation for Prediction of Aerodynamic Particle Size Distribution

A simple mass balance calculation combined with the definition of the aerodynamic diameter for a single drying droplet containing dissolved solid phases can be used to calculate the aerodynamic diameter of the resultant dry particle:

$$d_{\mathrm{a}} = \sqrt[6]{\frac{\rho_{\mathrm{p}}}{\rho^*}}\sqrt[3]{\frac{c_{\mathrm{f}}}{\rho^*}}d_{\mathrm{d}} \tag{6}$$

where d_{a} is the aerodynamic diameter, ρ_{p} is the dry particle density, ρ^* is the reference density (1,000 mg/mL), c_{f} is the concentration of solids in the feed solution, and d_{d} is the atomized droplet diameter (18). Here both the droplet and the dry particle are assumed to be spherical, and Cunningham's correction for non-continuum behavior is assumed to be unity. These assumptions are reasonable for most spray-dried inhalable formulations. Since solutes are dissolved they may be assumed to be uniformly distributed throughout the atomized spray, and thus utilizing the mass median droplet diameter in this equation gives an approximate prediction for the resulting mass median aerodynamic diameter (MMAD) of the dried particles. To utilize this relationship for spray-dried powders, the droplet size distribution produced by the atomizer must be known.

Lung Simulation Model

To estimate the amount of therapeutic agent delivered regionally within the lungs, a one-dimensional dynamical lung deposition model was used to simulate the deposition of the spray dried particles in each generation of a model respiratory tract (19). This was combined with a model for the volume of airway surface liquid in each lung generation (20). The resulting *in silico* prediction model provides an estimate of the concentration of D-amino acids in the airway surface liquid throughout the tracheobronchial region. Further details of this model are given in section "Simulated Lung Deposition of D-Amino Acid Formulations".

The numerical prediction of D-amino acids concentration in the different generations of the airway surface liquid performed in the current study allows predictions of whether the aerosolized spray-dried powders will result in sufficient D-amino acid concentrations in the lungs to achieve antimicrobial effects. Such predictions are useful in guiding iterations to formulation design.

Formulation Targets

A key step of formulation design is the identification of the target formulation characteristics; once defined, these targets may be used as inputs in the aforementioned models, with process and formulation parameters as outputs. In this study, two formulations were selected for design and manufacture: D-Leu/D-Met/D-Trp/D-Tyr ('quaternary D-amino acid formulation'), and D-Leu/D-Met/D-Trp ('ternary D-amino acid formulation'). The two formulations were also chosen to demonstrate the robustness of the models, capable of adjusting process parameters in response to changes in formulation composition, while still achieving formulation targets. A list of the targets discussed in this section is described in Table I.

Formulation Composition

As mentioned in the introduction, the effective *in vitro P. aeruginosa* biofilm dispersing concentration claimed by Kolodkin-Gal *et al.* was 5 nM for each of the four D-amino acids (15). For the purposes of this study, this was assumed to be the estimated effective dosage at the airways' surface. Ideally, the

Table I Summary of Formulation Targets for the Quaternary and Ternary D-Amino Acid Formulations

Design targets
1. D-amino acid concentration throughout the lung airways is in great excess of 5 nM
2. Biopharmaceutical stability and protection • Amorphous trehalose in formulation
3. Primary particle size is 2–3 μm
4. Powders have high dispersibility • Rugose, hollow particles • Crystalline D-Leu behaves as dispersibility agent (> 0.20 mass fraction)
5. Efficient delivery of dry powder aerosol to the lung • > 40% *in vitro* lung dose fraction

quaternary D-amino acid formulation would have an amino acid content which far exceeds that which is required to deliver 5 nM per D-amino acid to the airways surface liquid (Design Target #1).

As the Aerolizer dry powder inhaler was the chosen device for this work, the following was assumed: a) a loaded dose of 20 mg; b) at least 25% of that loaded dose is delivered into the lungs; and c) a lung sputum volume of 10 mL (i.e. dissolution volume), based on an estimate of mucus production per day for a healthy human subject (21). Given these assumptions, each D-amino acid must comprise at least 0.1% by mass of the dried powder to achieve the minimum effective dosage. Trehalose dihydrate was selected as the bulking agent, on the basis that previous work has already been done to spray-dry trehalose and L-leucine (7), providing a foundation of data from which to proceed. In addition, in case a biotherapeutic were to be incorporated into this D-amino acid formulation at a future date, trehalose was also chosen for its protection against dehydration (Design Target #2) (22).

In Vitro Aerosol Properties

The critical powder quality attributes considered were the aerodynamic particle size distribution and the powder dispersibility. For drug delivery to the conducting airways and alveoli of the adult human lung, it is generally accepted that particles with an aerodynamic diameter of a few μm are required to achieve reasonable deposition efficiency (23, 24). Therefore, 2 μm was chosen as the target MMAD for the D-amino acid formulations (Design Target #3).

Good dispersibility of respirable particles leads to efficient aerosol delivery to the lung. For this study, efficient *in vitro* aerosol delivery was defined as transporting more than 40% of the loaded dose past the throat, and therefore into the lung (Design Target #5). L-Leucine (L-Leu) has been used as a dispersibility agent in dry powder formulations, provided that L-Leu constitutes at least a 0.20 mass fraction in the formulation to sufficiently encapsulate the particles (7, 25–27). There is evidence to indicate that D-Leu is also an effective dispersibility agent (28, 29), and based on these previous studies a D-Leu mass fraction >0.20 is a goal for formulation design (Design Target #4).

The efficiency of aerosol delivery to the lungs may also be influenced by particle morphology and particle density. Rugose particles have been shown to improve powder dispersibility by reducing cohesive forces due to lower contact surface area (30, 31). Powder dispersibility may also be improved by reducing particle density and thus increased geometric diameter for the same aerodynamic diameter, resulting in enhanced aerodynamic dispersion in DPIs (22). In this study, the two D-amino acid formulations will be required to have rugose, low-density particles for efficient *in vitro* aerosol delivery (Design Target #4).

Solid-State Properties

As discussed in subsection "Particle Formation Model", the particle formation model predicts that a solute component of a droplet which can crystallise during droplet drying, can form a crystalline shell and produce a hollow particle, provided that the solute mass fraction is sufficiently high to cover the surface. Given that D-Leu has been singled out as the dispersibility agent for the D-amino acid formulations, D-Leu must be crystalline in the final spray-dried particle (Design Target #4), in order to occupy the surface, and also form the low-density hollow particle which will collapse and become rugose (Design Target #4).

As stated in subsection "Formulation Composition", trehalose is an excipient which has been promoted as a protectant of biotherapeutic agents, such as peptides, proteins, gene therapy vectors, bacteriophages and vaccines (27, 32, 33). The proposed mechanism for protection is that amorphous trehalose provides a glassy vitreous state which prevents protein unfolding during dessication, thus maintaining biological activity for these compounds (22). Since the quaternary D-amino acid mixture has the potential to behave as an adjuvant to antibiotic therapy or biotherapeutics, the formulations in this study will be designed with a view to future inclusion of these compounds. Consequently, the trehalose in the ternary and quaternary D-amino acid formulations will need to be amorphous (Design Target #2).

Physical stability of amorphous pharmaceuticals can be achieved by aiming for a storage temperature at or below the Kauzmann temperature, which is the point where molecular mobility is reduced to a level which is no longer significant for pharmaceuticals (34, 35). The Kauzmann temperature is usually estimated to be 50K below the glass transition temperature (34)]. The dry glass transition temperature of trehalose dihydrate (~120°C) (36) is more than 50°C above room

temperature, making trehalose an ideal candidate for maintaining physical stability of the powder in storage.

MATERIALS AND METHODS

Materials

The D-amino acids (D-Leu, D-Met, D-Trp and D-Tyr) were purchased from Sigma Aldrich (Oakville, ON, Canada). Deionised ultra-filtered water, trehalose dihydrate and anhydrous methanol were purchased from Fisher Scientific (Ottawa, ON, Canada).

Application of Models to Formulation Targets

A Priori Predictions: Drying Kinetics and Particle Structure

For an inlet gas temperature of 90°C and 0%RH, the following was assumed for the calculation of Peclet number (Equation 1): an evaporation rate of 5.5 μm^2/ms (2); trehalose diffusion coefficient of 1×10^{-5} cm^2/sec (37), and D-amino acids diffusion coefficient of 7.35×10^{-6} cm^2/sec (38). The resulting particle formation parameters for the quaternary formulation are shown in Table II, where it is seen that the initial Peclet number for each of the D-amino acids in the ternary and quaternary formulations is less than 1, suggesting that the dried particles would be solid with evenly distributed components. However, if we consider saturation time, it is seen that D-Tyr, with the lowest aqueous solubility (~400 μg/mL), reaches saturation during droplet evaporation much earlier (0.96 ms, or 0.05 of total droplet lifetime) than trehalose or the other D-amino acids. D-Leu is the second component to reach saturation (at 0.68 of total droplet lifetime), followed by D-Trp, with D-Met and trehalose reaching saturation last.

From the calculated particle formation parameters, D-Tyr and D-Leu are expected to be crystalline, given their wide precipitation windows (0.32 normalised droplet lifetime for D-Leu, 0.95 for D-Tyr). The narrow precipitation window for trehalose suggests that it will remain amorphous for both ternary and quaternary D-amino acid formulations. D-Met may be amorphous, since its precipitation window is similar to trehalose. The data is insufficient to predict whether D-Trp will be crystalline. The only anticipated difference in particle formation between the ternary and quaternary formulations is the lack of crystalline D-Tyr in the ternary formulation.

In terms of the particle formation process (Fig. 2), the early crystallization of D-Leu is anticipated to result in high surface enrichment, and the creation of a crystalline shell. Although D-Tyr crystallises much earlier, it only constitutes 3.3% of the quaternary D-amino acid formulation, and is not likely to affect D-Leu shell formation. As the liquid phase continues to reduce in volume, the trehalose forms an amorphous layer beneath the D-Leu shell. The final dry particle is expected to contain an internal void space.

Table II Particle Formation Parameters Calculated for the Quaternary D-Amino Acid Formulation, From a Mechanistic Model of Multi-Component Droplet Evaporation

Component	Peclet number (*Pe*)	Droplet lifetime (t_D; ms)	Normalised saturation time (t_{sat}/t_D)	Normalised precipitation time (t_p/t_D)
Trehalose	1.375	19.67	0.95	0.05
D-Leu	0.942		0.68	0.32
D-Met	0.942		0.94	0.06
D-Trp	0.942		0.88	0.12
D-Tyr	0.942		0.05	0.95

A Priori Calculation: Spray Dryer Atomizing Conditions

Given the target dry particle MMAD of 2 μm, Eq. 5 provides a means of estimating required droplet diameter for a given solids concentration. However, the dependence of droplet diameter distribution on liquid and gas flow rates in the atomizer must be known. This was measured experimentally. A customized version of the twin fluid atomizer supplied with the Buchi B-191 lab scale spray dryer (Büchi Labortechnik AG, Flawil, Switzerland), with a liquid nozzle diameter of 0.33 mm, and an annular gas nozzle of 1.63 mm outer diameter and 1.45 mm inner diameter, was tested. This nozzle was fitted to a modified Buchi B-191 spray dryer equipped with sampling ports for real time aerodynamic particle sizing of the aerosol and post-process analysis of particle morphology by scanning electron microscopy (see subsection "Focused Ion Beam (FIB) Milling and Scanning Electron Microscopy (SEM)").

A test aerosol with solid, spherical particles was produced to indirectly measure atomized droplet diameter distribution. An aqueous solution of trehalose at 60 mg/mL dissolved solids was prepared, supplied to the atomizer with a syringe pump (PHD Ultra, Harvard Apparatus, Holliston, MA, USA), and sprayed at varying atomizing conditions—air-liquid ratios (defined as the ratio of the gas and liquid mass flow rates) from 2 to 15 and liquid flow rate at 2.5, 5.0 and 7.5 mL/min. Drying conditions were then chosen to maintain a low Peclet number for trehalose in order to produce solid, spherical dry particles.

For each atomizing condition, the dried trehalose aerosol was sampled and the aerodynamic diameter was measured using a time-of-flight aerodynamic particle sizer (Model 3321, TSI, Shoreview, MN, USA) equipped with an aerosol diluter

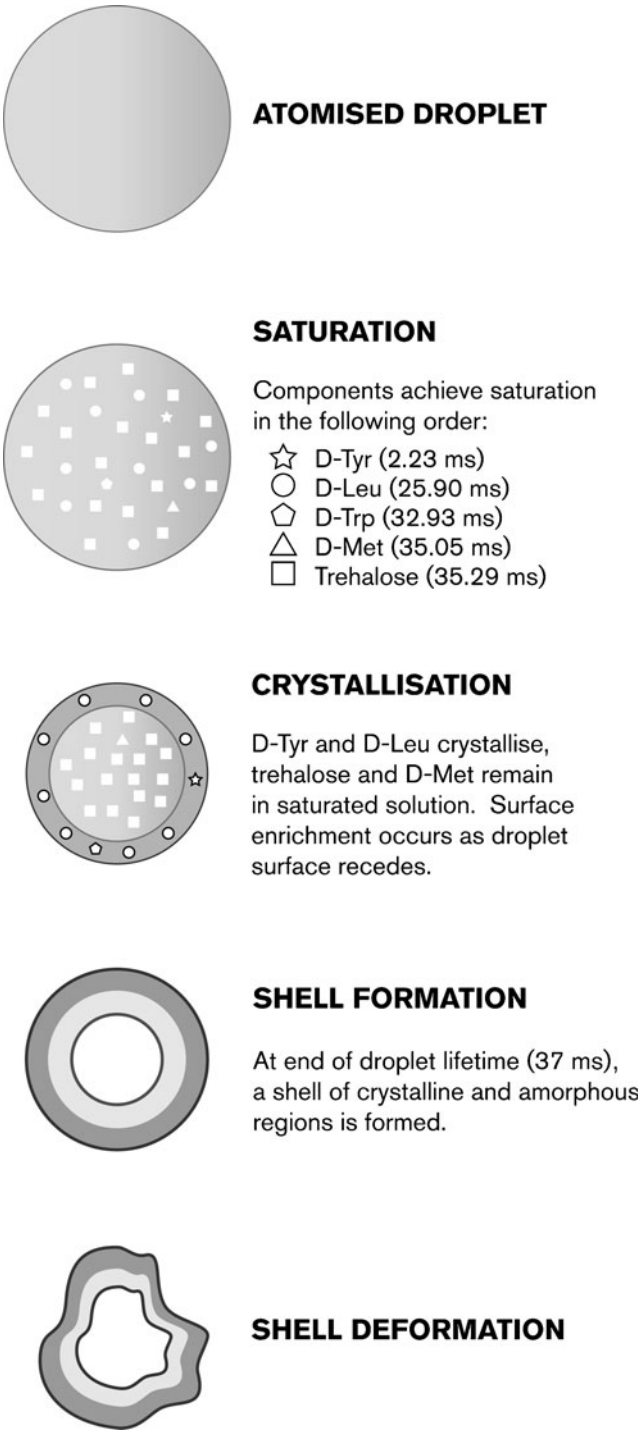

Fig. 2 Proposed particle formation process for atomized solution containing trehalose, D-Leu, D-Met, D-Trp and D-Tyr.

(Model 3302A, TSI, Shoreview, MN, USA) to dilute the aerosol to an appropriate range for the measurement (see subsection "Mass Median Aerodynamic Diameter (MMAD)"). Measurements were performed in duplicate. The measured aerosol MMAD and known solids concentration were used to calculate an approximate atomized droplet mass median diameter by rearrangement of Equation 6:

$$d_{\mathrm{d},50} = \sqrt[6]{\frac{\rho^*}{\rho_{\mathrm{p}}}}\sqrt[3]{\frac{\rho^*}{c_{\mathrm{f}}}}d_{\mathrm{a},50} \tag{7}$$

where $d_{\mathrm{d},50}$ is the atomized droplet mass median diameter and $d_{\mathrm{a},50}$ is the aerosol MMAD. It should be noted that a particle density value must be assumed to use this equation; in this case, it was assumed that the particles were solid spheres with a particle density equal to the true density of crystalline trehalose—1,520 mg/mL (47). The results of these experiments are plotted in Fig. 3. The droplet mass median diameter decreases with increasing air-liquid ratio. There appears to be some dependence on liquid flow rate, with the lowest liquid flow rate of 2.5 mL/min producing a slightly larger droplet mass median diameter for a given air-liquid ratio.

To check the assumption of solid, spherical particles (which could introduce uncertainty in the calculations using Eq. 7), a powder sampler was used to sample dried particles onto an SEM stub for the condition with the largest Peclet number of 1.375. A micrograph of these particles appears in Fig. 4; while it is not possible to definitively determine whether or not the particles have internal voids from the micrograph alone, the high sphericity of the particles indicates at worst a thick-shelled morphology. Due to the 1/6th power dependence of the calculated droplet mass median diameter on the particle density (Eq. 7), the calculated droplet median diameter values are relatively insensitive to variations in the assumed particle density.

The known dependence of the atomized droplet diameter distribution on air-liquid ratio and spray rate, in combination with Eq. 6, allows *a priori* determination of appropriate

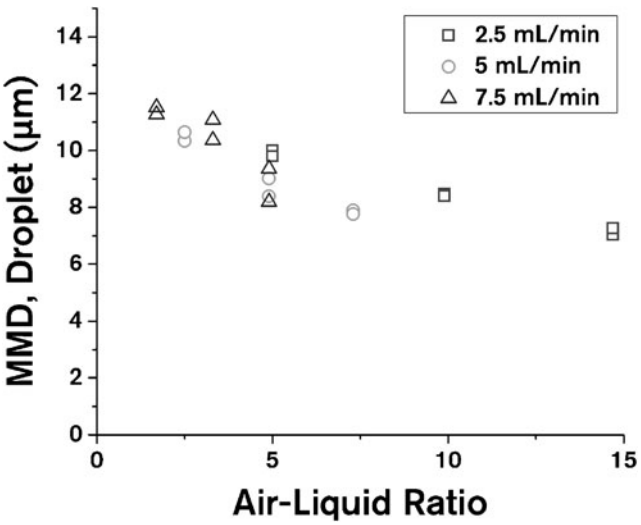

Fig. 3 Calculated atomized droplet diameter versus atomizer air-liquid ratio for tested liquid flow rates. The different symbols correspond to different liquid flow rates: squares 2.5 mL/min, circles 5.0 mL/min, triangles 7.5 mL/min.

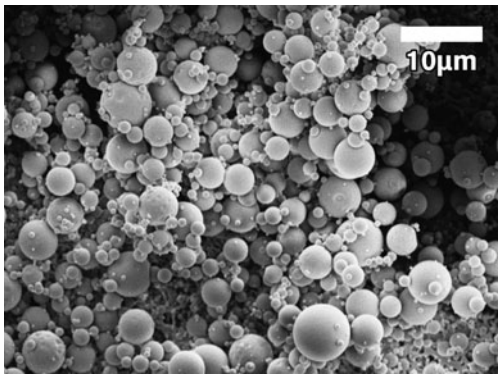

Fig. 4 SEM image of spray dried trehalose particles sampled during the atomizer droplet size determination experiment. The drying condition with the highest Peclet number (1.375) is shown.

atomizing conditions to meet targets on dry particle MMAD for a given solution feedstock. However, any atomizer has inherent constraints on attainable spray rates and gas-liquid ratios. A careful consideration of these constraints will guide the design of formulation composition and spray drying process parameters.

Spray Drying of Ternary and Quaternary D-Amino Acid Formulations

Two aqueous solutions of trehalose (Tre) with D-amino acids were prepared for use as feedstocks for the spray dried powders—Tre/D-Leu/D-Met/D-Trp (ternary formulation) and Tre/D-Leu/D-Met/D-Trp/D-Tyr (quaternary formulation). Prior experience with trehalose-leucine formulations demonstrated that leucine mass fraction needs to exceed 0.20 for leucine to act as an effective dispersibility agent (7). A mass fraction of 0.30 was selected for D-Leu in both formulations (Design Target #4), while trehalose content was maintained at 0.60 mass fraction (Design Target #2), leaving 0.10 mass fraction for the remaining D-amino acids. Meanwhile, the minimum D-amino acid mass fraction for an effective dosage at the lung surface has been estimated to be 0.001 (subsection "Formulation Composition"). This allows for considerable overage in D-Met, D-Trp and D-Tyr content in the dry powder formulations.

The individual D-amino acid solution concentrations in the spray dryer feedstock were then maximized for throughput. However, due to the low aqueous solubility of D-tyrosine (~400 µg/mL after 3 hrs of sonication at 30°C; experimentally determined), D-Tyr content in the quaternary formulation was limited to less than 400 µg/mL and the overall feed concentration (c_f) was constrained to 10 mg/mL. As discussed in subsection "*A Priori* Calculation: Spray Dryer Atomizing Conditions", with a set feed concentration and target MMAD, the atomized droplet median diameter is manipulated by adjustment of the air-liquid ratio, to achieve the target primary particle size. Aqueous concentrations and calculated dry mass fractions are shown in Table III. Solutions were stirred with magnetic stirrers on a stir-plate for 12 h prior to spray drying; complete dissolution was verified by visual inspection—clear solutions resulted in both cases.

The spray drying conditions were chosen with some parameters remaining constant between the two formulations. Solutions were spray dried on a modified Buchi B-191 spray dryer (Buchi Labortechnik AG, Flawil, Switzerland), and powders were collected with a custom glass cyclone. Drying gas was supplied with an inlet temperature of 90°C at a flow rate of 425 standard L/min; solution was sprayed at 3.0 mL/min, with resultant outlet temperature of 44–45°C and predicted outlet RH of ~10%.

Assuming a particle density of 500 mg/mL (2), and taking into account the different feed concentrations of the two formulations , the required atomized droplet mass median diameter was calculated to be 7.5 µm for the ternary formulation, and 10.4 µm for the quaternary formulation. Using the experimental relationship determined between atomized droplet size distribution and air-liquid ratio (subsection "*A Priori* Calculation: Spray Dryer Atomizing Conditions"), the calculated atomizer air-liquid ratio for the ternary formulation was 12.6, and 3.6 for the quaternary formulation.

Simulated Lung Deposition of D-Amino Acid Formulations

The *in vitro* NGI deposition data (collected in subsection "Ambient Laboratory Conditions") was used to estimate aerodynamic particle size distribution. It was assumed that there were no particle size changes due to condensation of water vapour (i.e. non-hygroscopic assumption was made). The first step of the simulation was to calculate the spatial distribution of particles in the tracheobronchial region as described by Javaheri *et al* (19)., assuming the following breathing pattern: 2,000 cm (3) tidal volume, 60 L/min inhalation flow rate, 2 s inspiration time, 1 s respiratory hold time, and 3 s expiration

Table III Summary of Component Concentrations in the Spray Dried Formulations

Formulation (Total feed concentration in mg/mL)	Components (Aqueous concentration in mg/mL) [Dry powder mass fraction]				
	Trehalose	D-Leu	D-Met	D-Trp	D-Tyr
Ternary (27.0)	(16.2) [0.60]	(8.1) [0.30]	(1.4) [0.050]	(1.4) [0.050]	–
Quaternary (10.0)	(6.0) [0.60]	(3.0) [0.30]	(0.33) [0.033]	(0.33) [0.033]	(0.33) [0.033]

time, with a functional residual capacity (FRC) of 3,000 cm (3). For modeling deposition, equations for inertial impaction (39), sedimentation (40, 41), and diffusion (42) in each lung generation were used. Since the Alberta Idealized Throat was used as the induction port on the NGI, no extrathoracic deposition modeling was needed. Once the deposition distribution in each generation of the lungs was predicted, the D-amino acid concentrations in the airway surface liquid (ASL) were calculated for each tracheobronchial generation; this simulation is described in further detail elsewhere (20). The concentrations were calculated for three CF mucus conditions associated with different combinations of tracheal mucus velocity (in mm/min) and mucus production rates (mL/day), that are expected to span the *in vivo* range of airway surface liquid concentrations (20). The three conditions were: 1) Low concentration (5 mm/min, 20 mL/day); 2) Medium concentration (12 mm/min, 10 mL/day); and High concentration (20 mm/min, 5 mL/day).

Mass Median Aerodynamic Diameter (MMAD)

The Aerodynamic Particle Sizer (Model 3321; TSI, Shoreview, MN, USA) determined the aerodynamic particle size distribution of each formulation. Approximately 5 mg of powder was loaded into the Small Scale Disperser Unit (Model 3433; TSI, Shoreview, MN, USA); the sample was entrained into the Venturi air flow and entered the APS at 5 L/min air flow rate. Each sample was measured for 20 s, and the results converted by the APS into a mass median aerodynamic diameter (MMAD) value. This was repeated five times for each formulation.

Modulated Differential Scanning Calorimetry (mDSC)

The Differential Scanning Calorimeter (Model Q1000; TA Instruments, New Castle, DE, USA) was used for thermal analysis of the formulations. Approximately 3–4 mg of a sample was weighed into a hermetic aluminium pan; two holes were punched through the hermetic aluminium lid with a needle, before crimping pan and lid together. The modulated DSC method was as follows: modulation ±0.618°C /min, equilibration at 20°C for 30 mins, and temperature ramp from 20 to 180°C at 2°C/min.

Focused Ion Beam (FIB) Milling and Scanning Electron Microscopy (SEM)

Samples were mounted onto aluminium SEM stubs, and gold sputter-coated (Nanotech SEMprep 2, Prestwick, UK) to a thickness of 150Å. Images of the spray-dried particles were captured with Field Emission Scanning Electron Microscope (JEOL Model JSM-6301 FXV, Tokyo, Japan).

The Zeiss NVision 40 Focused Ion Beam-Scanning Electron Microscope (FIB-SEM; Carl Zeiss, Oberkochen, Germany) was used to section quaternary D-amino acid particles and investigate the internal structure. Samples were mounted onto aluminium SEM stubs fitted with a 400 mesh Cu grid. The samples were gold sputter-coated (Model 682 Precision Etch Coating System; Gatan Inc., Abingdon, UK) to a thickness of 50 nm. FIB milling with a gallium beam was conducted with 30 kV voltage and 80 pA current.

Raman Spectroscopy

Raman spectroscopy was used to explore the solid state of the spray dried powders. A custom built dispersive low-frequency shift Raman setup was used to measure the Raman spectra of different amino acids. The setup includes an argon Ion Laser (514.5 nm) with a triple filter stage for laser line rejection, and a cryogenically-cooled CCD sensor with a spectral resolution of ~1 cm^{-1}. A detailed description of the setup, including calibration and methodology, can be found in previous publications (7, 43, 44). This setup has the advantage of low sample mass requirements (~0.5 to 5.0 mg) (45), and has been used successfully for the study of leucine (44) and trehalose-leucine (7) systems.

Bulk Powder Density

Conventional tapped density techniques, which require a sample mass typically in the range of several grams, are of questionable use for respirable powders where inter-particulate forces dominate over the gravitational force. An alternative technique of Compressed Bulk Density measurement (46) is applied in this study, using a precise instrument that applies a dynamic low-pressure compaction on a powder bed (within the range of 0 to 1 MPa). This technique determines the density of a powder under a defined compaction pressure, requiring only milligrams of powder. A cylindrical sample pan with a known volume is filled loosely with a known mass of powder and is placed on a 10 lb loadcell (LRF400; FuTeK, Irvine, CA, USA), while a 25 mm non-rotary, linear actuator (M-229.26S; Physik Instrumente, Irvine, CA, USA) drives a disk shape punch into the cavity. The compressed bulk density tester is interfaced with LabVIEW v. 2011 (National Instruments, Austin, TX, USA) to communicate with the measuring articles as they record the real time pressure, exerted on a powder surface, as a function of the changes in powder bed volume. The correlation between these values is shown on a force-displacement plot, as well as a plot of density versus compaction pressure. For the purposes of this study, compressed bulk density measurements were taken of the ternary and quaternary spray-dried powders across a pressure range of 0 to 1200 kPa. The measurements were normalised by the mass-weighted average of the majority component true

densities—1,580 kg/m^3 for trehalose (47) and 1,314 kg/m (3) for leucine (48).

In Vitro Aerosol Performance

Controlled Conditions

The two formulations were tested in a setup designed for controlled ambient conditions (Fig. 5). The Alberta Idealised Throat (49) was connected to a filter (Respirgard TM II 303, Vital Signs Devices, Totowa, NJ, USA). Both the throat and filter were kept within an environmental chamber (Model CE0910W-4, Lunaire, Williamsport, PA, USA), and the filter outlet was joined to a rotary vane vacuum pump (Gast Manufacturing, Michigan, USA). The throat was sprayed with silicone (Molykote® 316, Dow Corning, Midland, MI, USA) before each run. After assembling the throat and filter, the vacuum pump was adjusted to provide 60 L/min air flow at the throat mouthpiece; during adjustment, the airflow was monitored at the mouthpiece with a mass flowmeter (Model 4040, TSI, Shoreview, MN, USA). The spray dried powders were weighed and filled into gelatin capsules (20 mg per capsule) from within a glove box supplied with dry nitrogen gas (<1% RH). The capsule and dry powder inhaler (Aeroliser®DPI; Italseber Farmaceutici, Italy) were placed in a polycarbonate vacuum dessicator, vacuum-sealed, and transferred into the environmental chamber.

The environmental chamber was set to maintain ambient conditions at 20±2°C and 35±2% RH. The capsule and DPI were removed from the dessicator, and the capsule was loaded into the DPI before it was pierced. The DPI was inserted into the throat mouthpiece, and the vacuum pump switched on to disperse the powder at 60 L/min. The deposited powder was recovered with deionised ultra-filtered water, from the throat (10 mL) and filter (10 mL). The aerosolisation procedure was performed in triplicate for each of the formulations.

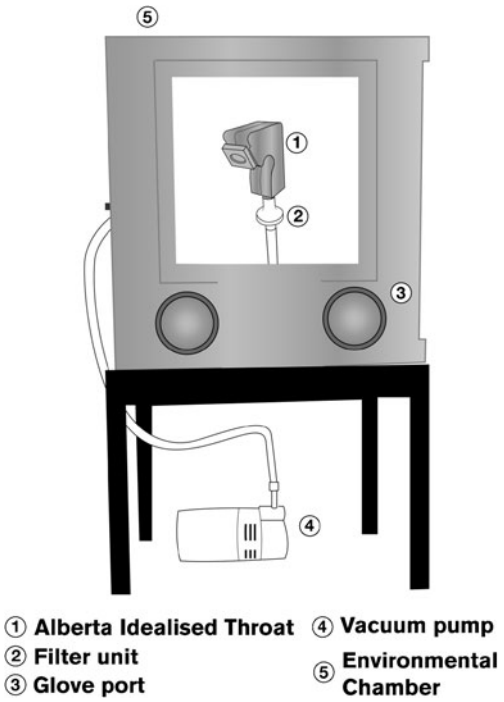

Fig. 5 Setup for *in vitro* aerosol performance testing in controlled conditions.

Ambient Laboratory Conditions

Another set of aerosolisation tests were conducted to provide aerodynamic particle size distribution data for the lung deposition model simulation (section "Simulated Lung Deposition of D-Amino Acid Formulations"), for the quaternary formulation. The setup for these tests is shown in Fig. 6. The Alberta Idealised Throat (AIT) was connected directly into the Next Generation Impactor (NGI; MSP Corporation, Shoreview, MN, USA) inlet, and the NGI was connected to the vacuum pump which was set to 60 L/min air flow rate. Both the throat and NGI stages were sprayed with silicone oil prior to each run. As with the aerosolisation tests in controlled conditions, the capsules were filled and the Aeroliser loaded in the dry glove box (< 1% RH). However, the powders were dispersed from the Aeroliser into the NGI in ambient laboratory conditions (22.6±0.60% RH, 21.9±0.1°C). The deposited powder was recovered from the throat and each NGI stage with 10 mL deionized water. The aerosolisation run was performed in triplicate. All recovered samples from the controlled and ambient conditions aerosolisation tests were assayed for D-amino acid content by UV spectrophotometry (see section "UV Spectrophotometry").

UV Spectrophotometry

The ninhydrin reaction was used for colorimetric assay by UV spectrophotometry (HP 8452 Diode Array Spectrophotometer; Agilent Technologies, Santa Clara, CA, USA). However, all four D-amino acids react with ninhydrin, producing Ruhemann's Purple (absorbance maxima 570 nm); consequently, only total D-amino acid content could be determined by this assay. This assay was tested on bulk quaternary formulation powder samples (mass 20 mg, $n=2$), which found total D-amino acid content to be 104–105% of theoretical content.

To deconvolute total D-amino acid content into individual content, the collective amount of D-Trp and D-Tyr (both aromatic amino acids) in the rinsates were determined separately from the ninhydrin assay, using a glass cuvette (PCS 1115; Malvern Instruments, Worcestershire, UK) instead of quartz, and measuring UV absorbance at 278 nm. This method was tested on bulk quaternary formulation powder samples (mass 20 mg, $n=2$), which found D-Tyr and D-Trp content to be 99–100% of theoretical content. Thus the total

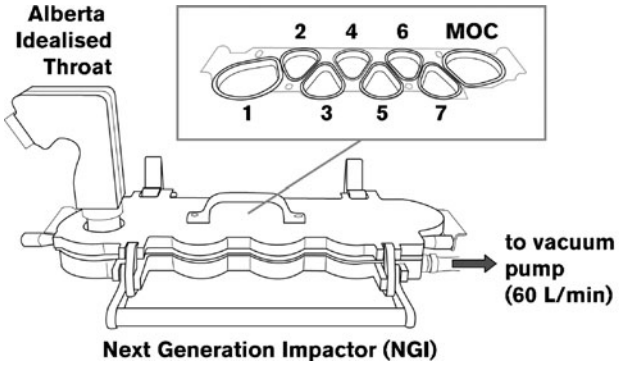

NGI STAGE	AERODYNAMIC CUT-OFF DIAMETER (μm)
1	8.06
2	4.46
3	2.82
4	1.66
5	0.94
6	0.55
7	0.34

Fig. 6 *In vitro* aerosol performance test setup in laboratory conditions. Inset shows the NGI collection stages 1–7, and micro-orifice collector (MOC).

D-amino acids and D-Tyr/D-Trp UV spectrophotometric assays were concluded to be reliable.

By subtracting D-Tyr/D-Trp content from total D-amino acids content, we were able to determine D-Leu/D-Met content. Since the composition of the formulations are already known, these collective contents can be further broken down into individual D-amino acid contents.

Calculations and Statistical Analysis

In vitro aerosol deposition results were calculated from the aerosolisation efficiency studies in the AIT/filter and NGI setups. The powder mass weighed into the gelatin capsule was taken to be 'loaded dose', and the total amino acid mass per dose (i.e. 40% of loaded dose) was taken to be 'loaded amino acid dose'. Total amino acid deposition in the filter, or in the NGI stages, distal to the AIT was taken to represent 'lung dose', and the amount of powder recovered ex-device was taken to represent 'emitted dose'. The throat deposition and lung dose of both formulations were also expressed as a percentage of loaded amino acid dose.

For the NGI deposition tests another parameter, mass median aerodynamic diameter for lung dose ($MMAD_{lung}$), was calculated by plotting a lognormal cumulative mass undersize plot corresponding to NGI stage particle size fraction, and applying linear regression to the plot. This gave an estimate of the mass median aerodynamic diameter for the fraction of aerosol which passed through the Alberta Idealised Throat, and reached the stages of the impactor.

Primary particle size and *in vitro* throat and lung deposition results were analysed using Student's unpaired t-test; statistically significant difference was reported where p-value < 0.05.

RESULTS AND DISCUSSION

Aerodynamic Particle Size Distribution

When measured by the APS (time-of-flight light scattering method), mass median aerodynamic diameter (MMAD) was 2.09 ± 0.14 μm for the ternary D-amino acid formulation, and 2.60 ± 0.05 μm for the quaternary D-amino acid formulation (significantly different; $p < 0.0005$). The particle size distributions were unimodal, with a geometric standard distribution of 1.80 ± 0.09 for the ternary formulation, and 1.70 ± 0.14 for the quaternary formulation (not significantly different; $p > 0.1$). It should be noted that in order to determine the MMAD of the primary particle, measurements of dry powder samples with the APS are reliant upon the complete dispersion of the powder, which may not have occurred here.

With the measured MMAD close to 2 μm, the formulations achieve Design Target #3. This result also confirms that with an established experimental relationship between feed flow rate, air-liquid ratio and atomized droplet diameter for the spray dryer system to be used (section "*A Priori* Calculation: Spray Dryer Atomizing Conditions"), the spray dryer process model can successfully predict the process parameters required for the manufacture of a target particle diameter.

The quaternary formulation aerodynamic diameter distribution by mass of the aerosol that passed the Alberta throat model measured in the NGI is depicted in Fig. 7. All four D-amino acids showed peak deposition in Stages 3 and 4 (0.94–4.46 μm) with a gradual decline in deposition on the lower stages. D-Leu deposition ranged from 80 to 700 μg per stage, while D-Met, D-Trp and D-Tyr deposition ranged from 10 to 90 μg per stage.

The $MMAD_{lung}$ for the quaternary formulation was calculated to be 1.76 ± 0.14 μm. One of several explanations for this value being lower than the primary particle MMAD measured by the APS (statistically significant; $p < 0.00005$) may be the collection of larger particles in the Alberta Throat. In comparison, the APS measured the primary particle size of a dispersed powder sample, without any kind of pre-separation stage placed before the APS inlet.

Solid State Properties and Particle Morphology

The mDSC traces show that both ternary and quaternary formulations have an obvious glass transition (T_g) at ~119°C, corresponding to amorphous trehalose (Fig. 8). D-Leu appears

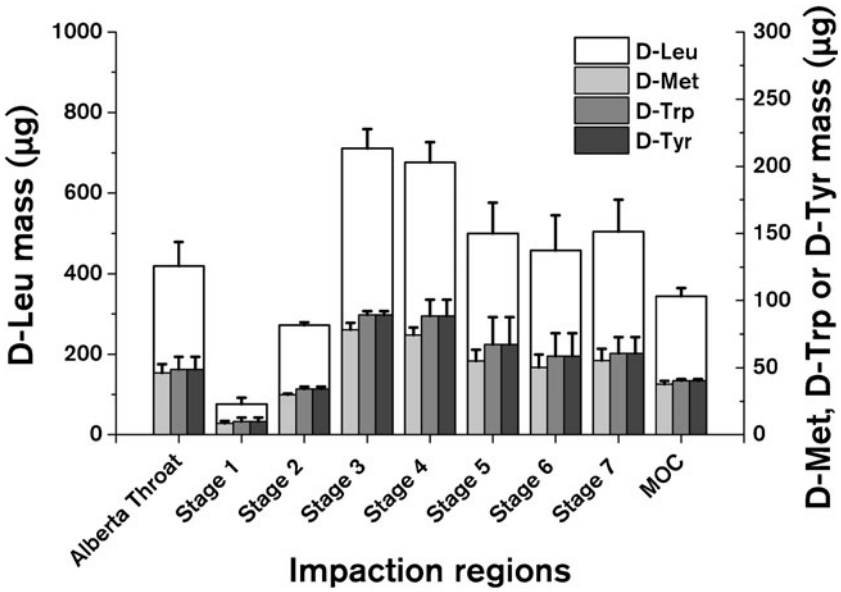

Fig. 7 Mass distribution of D-Leu (*left* y-axis) and D-Met, D-Trp and D-Tyr (*right* y-axis) in the Alberta Idealised Throat and NGI stages after dispersion of the quaternary D-amino acid formulation from an Aeroliser DPI at 60 L/min ($n = 3$).

to be crystalline, given that it constitutes 30% of the formulation composition and there is no indication of a glass transition region. These results satisfy Design Targets #2 and #4. However, the ternary formulation has a deviation in the mDSC trace within the 95–110°C region. Furthermore, there is no equivalent deviation in the mDSC trace for the quaternary formulation. A previously tested Tre:D-Met (80:20) spray-dried formulation revealed a glass transition at 100°C (unpublished data), and it is possible that the mDSC is not sensitive enough to detect a glass transition for amorphous D-Met when it only constitutes 3.3% of the formulation composition, and when it constitutes 5% (such as in the ternary formulation) there is only a slight baseline deviation. There is also the possibility that D-Tyr or D-Trp are also amorphous, with glass transitions overlapping that of D-Met, and thus we are unable to definitively conclude the microstructure of the formulations by mDSC alone.

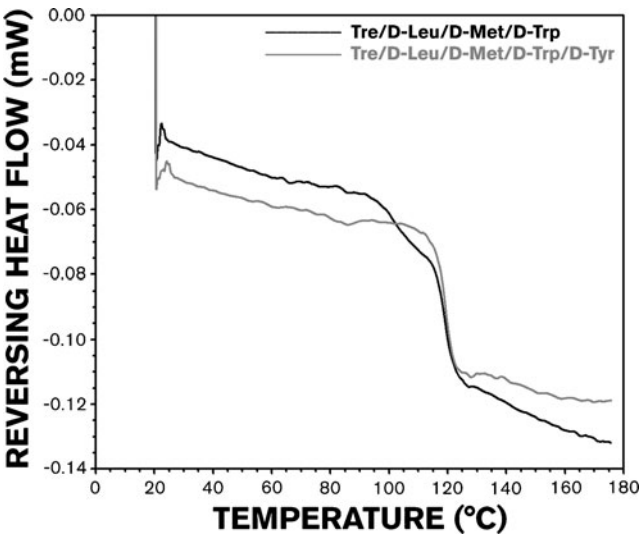

Fig. 8 Modulated DSC traces for the ternary (black line) and quaternary D-amino acid formulation (grey line).

For this reason, we analyze the low-frequency Raman spectra. The reference spectra for amorphous trehalose, amorphous D-Met, crystalline D-Leu, crystalline L-Leu, and crystalline D-Tyr are shown in Fig. 9, while the Raman spectrum for the quaternary formulation is shown in Fig. 10 (top panel). The spectrum for D-Leu in the formulation is indistinguishable from that of crystalline L-Leu, supporting the hypothesis that D-Leu will likely behave as a dispersibility agent.

The reference spectra for the majority components (amorphous trehalose and crystalline D-Leu) were subtracted from the quaternary D-amino acid Raman spectrum in Fig. 10, leaving a residual spectrum (Fig. 10, bottom panel). The low normalized intensity in the residual spectrum indicates that trehalose is amorphous, and D-Leu is crystalline, within the quaternary formulation, as predicted by the particle formation model.

The solid state of the remaining components (D-Met, D-Trp and D-Tyr) could not be confirmed due to their low mass fraction (3.3%) which is within the detection limit of the used Raman setup. Comparing the residual spectrum to the D-Met crystalline spectrum suggests that D-Met is more likely to be amorphous since the residual spectrum does not show any of the significant peaks in the crystalline form. A reference spectrum for amorphous D-Tyr could not be obtained, however a sharp peak at around 850 cm^{-1} in the residual spectrum and the crystalline D-Tyr spectrum suggest that D-Tyr is crystalline. D-Trp reference spectra could not be measured by Raman spectroscopy due to interference by sample fluorescence, and its precipitation window (4.07 ms) falls in between that of D-Met (amorphous) and D-Leu (crystalline). As a result, the solid state of D-Trp remains unconfirmed.

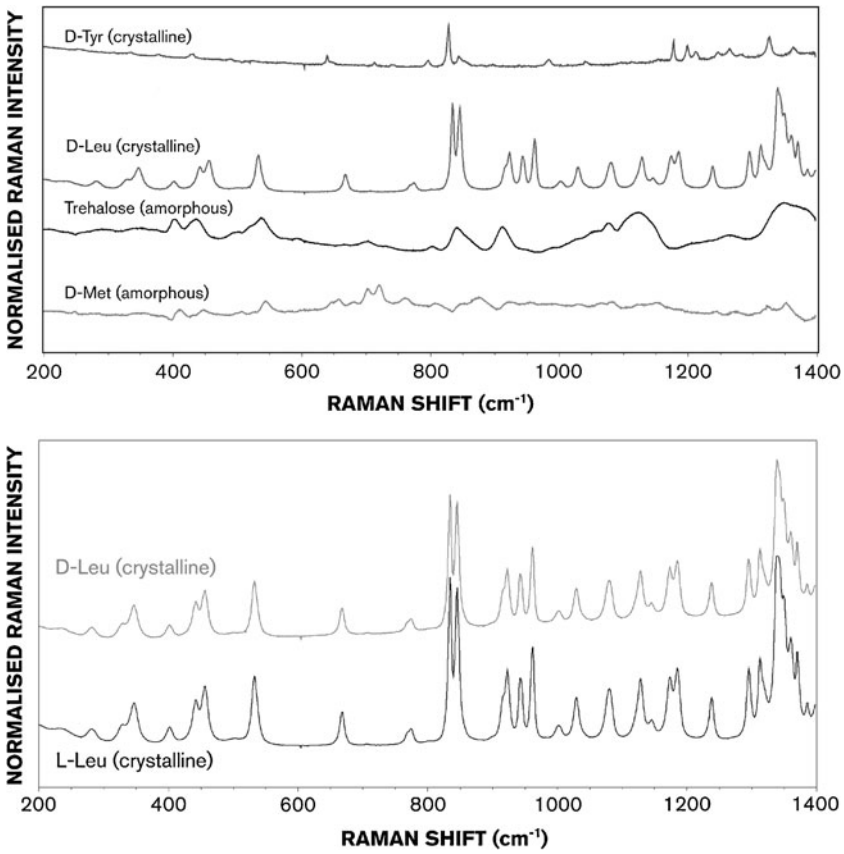

Fig. 9 Low-frequency Raman reference spectra for trehalose, D-Leu, D-Met and D-Tyr (*top*); a comparison of crystalline D-Leu and L-Leu Raman reference spectra (*bottom*).

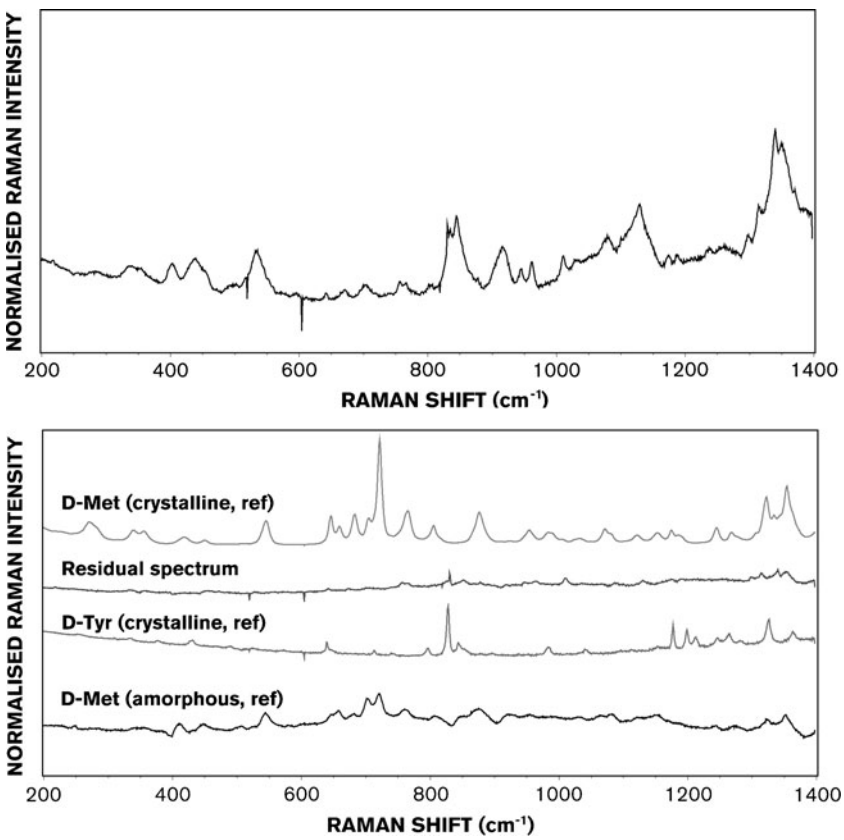

Fig. 10 Raw spectrum (*top*) and residual spectrum (*bottom*) for the quaternary spray-dried formulation.

Identification of amorphous trehalose, amorphous D-Met, crystalline D-Leu and crystalline D-Tyr within the quaternary D-amino acid formulation supports predictions made from the particle formation model—that D-Leu and D-Tyr were able to crystallise within the precipitation window, while trehalose and D-Met were not (section "*A Priori* Predictions: Drying Kinetics and Particle Structure").

The particle morphology of the spray-dried particles also supports the particle formation model. With D-Leu and D-Tyr predicted to crystallize during droplet evaporation, their Peclet numbers increase dramatically as a result of their reduced mobility in the solvent. High surface enrichment results and a predominantly D-Leu crystalline shell is formed; after the particle is formed, the shell may deform or collapse (Fig. 2). SEM images of the spray dried particles are shown in Fig. 11, and both ternary and quaternary formulations have rugose particles, indicating that the predicted shell formation and collapse has occurred.

The normalized compressed bulk density was approximately 0.3 to 0.5 across the tested pressure range. If the powders consist of solid particles, we may expect normalized compressed bulk density to be close to 0.6–0.7, assuming random packing of the polydisperse spherical particles (50). The low compressed bulk density results indicate the presence of internal void space or porous material.

Additional confirmation of our predictions of the internal structure of the particles comes from the FIB-SEM images (Fig. 12). The images clearly show a shell layer and internal void space for larger particles (2–3 μm geometric diameter), while smaller particles (~1 μm or less) were solid throughout. This is consistent with particle formation theory, as smaller atomized droplets would have shorter droplet lifetimes, and since saturation and precipitation times are proportional to droplet lifetime (Eqs. 4 and 5), there is less time for components to crystallise and form a shell.

The manufacture of multi-component spray-dried particles in this study clearly demonstrates particle formation theory in action, where alterations to the kinetics of the individual components have consequences to the final particle microstructure. Application of the particle formation model to the ternary and quaternary D-amino acid formulations was successful in designing rugose and low-density particles, achieving Design Target #4.

If we look at the moisture sorption isotherm for amorphous trehalose (51), a predicted spray dryer outlet RH of 10% (section "Spray Drying of Ternary and Quaternary D-Amino Acid Formulations") corresponds to approximately 2% moisture content. D-Leu is crystalline and hydrophobic, and is unlikely to affect moisture sorption for the powders. Composite state diagrams for trehalose-water systems show that 2% moisture content (or 98% trehalose content) does not lower glass transition temperature sufficiently to raise stability concerns (51, 52). Thus, future biotherapeutic formulations which use this trehalose-D-amino acid formulation as a delivery platform are likely to maintain product stability—provided the powders are collected and stored at outlet RH, due to the high dry T_g of amorphous trehalose relative to room temperature.

In Vitro Aerosol Performance

The aerosolisation tests for controlled and ambient lab conditions are summarised in Table IV. For the quaternary formulation, the *in vitro* aerosol deposition results are similar after testing in both the Alberta Throat and Filter, and the NGI (no statistically significant difference in emitted dose, throat fraction or lung dose fraction; $p > 0.05$). The ternary formulation results show slightly lower emitted dose (53.75 ± 8.42%) and lung dose fraction (46.95 ± 6.89%) compared to the quaternary formulation, although this was not a statistically significant difference ($p > 0.05$).

As predicted by the particle formation model (Fig. 2), and supported by mDSC and Raman results, D-Leu crystallises during droplet drying; since D-Leu also constitutes 30% of the formulation composition, D-Leu would be expected to dominate the crystalline shell formed in the final particle. The

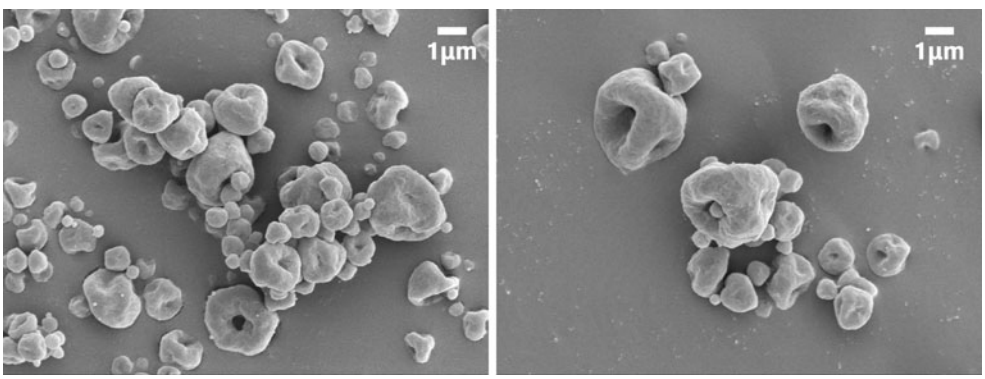

Fig. 11 SEM images of spray dried ternary (*left*) and quaternary (*right*) D-amino acid formulations.

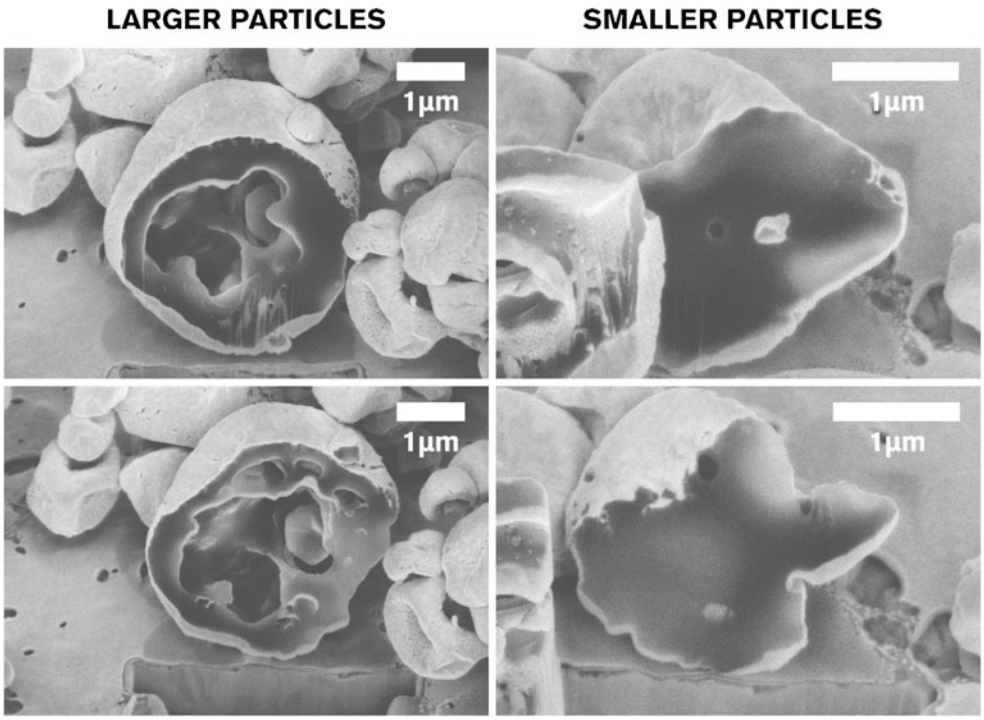

Fig. 12 Focused Ion Beam milled quaternary D-amino acid particles, with a third of the particle sectioned (*top*), and with half of the particle sectioned (*bottom*).

Raman spectra analysed in this study indicated no difference in microstructure between L- and D-Leu, and L-Leu is well known as a dispersibility agent for dry powder formulations, from which we hypothesised that the D-Leu in the quaternary and ternary formulations in the current study will also behave as a dispersibility agent.

The spray dried powders in this study did indeed demonstrate efficient delivery in both controlled and lab conditions (47% lung dose fraction for the ternary formulation, 56% for the quaternary formulation), considering that the powders were dispersed from a low-medium resistance DPI device ($0.055\ (cm.H_2O)^{1/2}/L.min^{-1}$ (53)). There was also no significant difference in lung dose fraction between the ternary and quaternary formulations, which was to be expected since D-Leu is the dominant D-amino acid component, while crystalline D-Tyr only constitutes 3.3% of the formulation. As such it was not expected to have an effect on powder dispersibility. The successful design and manufacture of rugose, low-density particles containing 30% w/w crystalline D-Leu (Design Target #4) results in dispersible ternary and quaternary D-amino acid formulations with high aerosol delivery efficiency (Design Target #5).

Simulated Lung Deposition of D-Amino Acid Formulations

Selected results of the lung deposition simulation are shown in Fig. 13, where the trachea is generation 0 and the terminal bronchioles are generation 14. Regardless of mucociliary clearance and mucus production rates, the highest airway surface liquid (ASL) concentrations were achieved with D-Leu (Fig. 13, left), and the lowest ASL concentrations were

Table IV Summary of *in vitro* Aerosol Performance Parameters for the Ternary And Quaternary Spray-Dried Formulations, Delivered from an Aeroliser DPI into the Alberta Throat/filter and NGI setups at 60 L/min

	Alberta throat and filter		NGI
	TRE/D-LEU/D-MET/D-TRP ($n=3$)	TRE/D-LEU/D-MET/D-TRP/D-TYR ($n=3$)	TRE/D-LEU/D-MET/D-TRP/D-TYR ($n=3$)
Loaded dose (mg)	20.17 (0.60)	20.59 (1.14)	21.07 (0.76)
Loaded amino acid dose (mg)	8.07 (0.24)	8.24 (0.46)	8.43 (0.30)
Emitted dose (%)	53.75 (8.42)	65.18 (8.00)	63.61 (4.30)
Throat fraction (%)	6.81 (1.70)	9.08 (1.36)	6.67 (1.26)
Lung dose fraction (%)	46.95 (6.89)	56.10 (7.15)	56.94 (4.27)

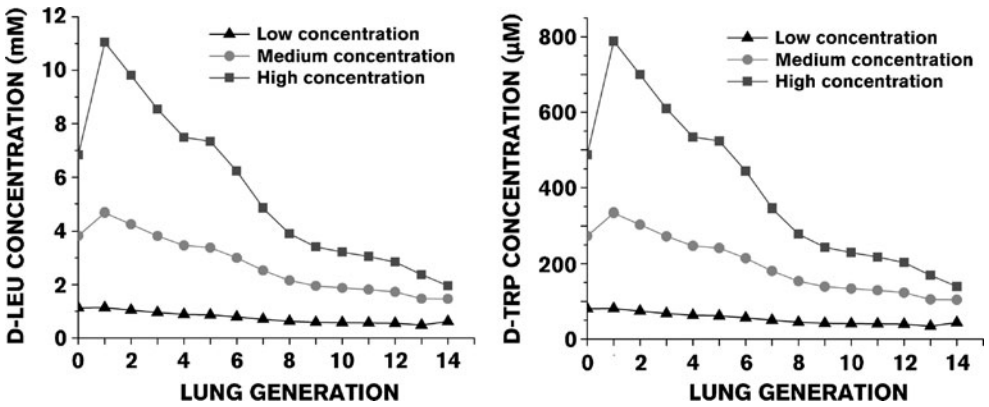

Fig. 13 Concentration of D-Leu (left) and D-Trp (*right*) deposited in lung generations 1-14, as predicted by mathematical lung deposition simulation. The distribution of deposited D-amino acids is shown for low (tracheal mucus velocity = 5 mm/min, mucus production = 20 mL/day), medium (tracheal mucus velocity = 12 mm/min, mucus production = 10 mL/day) and high concentration (tracheal mucus velocity = 20 mm/min, mucus production = 5 mL/day) conditions.

achieved with D-Trp (Fig. 13, right). D-Leu concentrations peaked at 11 mM (Generation 1, high concentration condition), and reached minimum at 0.48 mM (Generation 13, low concentration condition). D-Trp concentrations peaked at 788.5 mM (Generation 1, high concentration condition), and reached a minimum at 34.4 μM (Generation 13, low concentration condition).

As stated in the introduction, an equimolar quaternary D-amino acid solution was found to be an effective *P. aeruginosa* biofilm dispersing agent in an *in vitro* cell study (15). The composition of the quaternary D-amino acids formulation in this current study is not equimolar; thus, any assessment of adequate drug delivery should be based upon the lung delivery of components with the lowest content, which are D-Met, D-Trp and D-Tyr (3.3% w/w each). Of these, D-Trp resulted in the lowest concentrations in the lung deposition simulation (Fig. 13). However, even in the low concentration condition (mucus production 20 mL/day, mucociliary clearance 5 mm/min), the minimum D-Trp concentration achieved was 34.4 μM, far exceeding the 5 nM baseline target. Thus, the quaternary D-amino acid formulation achieves Design Target #1, and all the design targets have been accomplished. No further iterations to formulation design or the spray drying process are required.

On the other hand, any assumption of a real effective dosage achieved in the CF sputum from this simulation is of course uncertain, given that: a) the baseline target dosage of 5 nM was based upon *in vitro* cell work; b) the *in vitro* cell work was not performed in media reflective of CF sputum composition; and c) the lung simulation does not account for CF diseased lung morphology. Nevertheless, this lung deposition model is a helpful tool for assessment of respiratory drug delivery of antimicrobials, as an extension to the existing suite of pharmacopoeia aerodynamic particle size measurement methodologies.

CONCLUSIONS

This study demonstrates the utility of applying theoretical models to design a formulation and a spray drying process: given a set of design targets (aerodynamic diameter of 2–3 μm, high *in vitro* aerosol performance, simulated delivered lung dose in excess of 5 nM per lung generation), and some knowledge of the formulation components (solubility, diffusion coefficient), the appropriate formulation and process parameters were calculated *a priori*, with ease, and with no iteration necessary.

A second set of design targets may be selected to further improve the formulation and direct the first iteration of *in silico* process and formulation design—such as increasing emitted dosage, or adjusting target effective dosage on the basis of *in vitro P. aeruginosa* biofilm studies carried out with CF sputum . Consequently, experimental work is not eliminated with this approach, but in the context of complex formulations with design challenges—such as low aqueous solubility, multiple bioactive components, and a minimum target effective dosage—this approach demonstrates an advantage in time and resource cost over more traditional approaches (e.g. statistical design of experiments).

The successful production of both ternary and quaternary formulations also demonstrates the utility of current spray-drying model and particle formation theory, through the ability to adjust process parameters to achieve the same design targets despite the difference in formulation compositions. With novel bioactives and excipients becoming more expensive, a robust method which can minimize risk and time cost during formulation development is invaluable.

While the quaternary D-amino acid formulation was selected for the design challenges it posed to aerosol formulation development, this study also indicates that there is a real opportunity for the development of bioactive aerosols against bacterial biofilm infections in the lung, and it would be worth

considering the pursuit of other antimicrobial compounds for respiratory drug delivery.

ACKNOWLEDGMENTS AND DISCLOSURES

M. A. Boraey and R. Vehring would like to thank the Natural Sciences and Engineering Research Council of Canada (NSERC) and the Alberta Innovates Technology Futures (AITF) for their financial support.

REFERENCES

1. Weers JG, Bell J, Chan HK, Cipolla D, Dunbar C, Hickey AJ, *et al.* Pulmonary formulations: what remains to be done? J Aerosol Med Pulm Drug Deliv. 2010;23:S5–S23.
2. Vehring R, Foss WR, Lechuga-Ballesteros D. Particle formation in spray drying. J Aerosol Sci. 2007;38:728–46.
3. Nandiyanto ABD, Okuyama K. Progress in developing spray-drying methods for the production of controlled morphology particles: from the nanometer to submicrometer size ranges. Adv Powder Technol. 2011;22:1–19.
4. Dobry DE, Settell DM, Baumann JM, Ray RJ, Graham LJ, Beyerinck RA. A model-based methodology for spray-drying process development. J Pharm Innov. 2009;4:133–42.
5. Ivey JW, Vehring R. The use of modeling in spray drying of emulsions and suspensions accelerates formulation and process development. Comput Chem Eng. 2010;34:1036–40.
6. Boraey MA, Matinkhoo S, Vehring R. A new time and cost effective approach for the development of microparticles for pulmonary drug delivery. In: Dalby RN, Byron PR, Peart J, Suman JD, Young PM, editors. Respiratory drug delivery Europe, vol. 2. Davis Healthcare International Publishing: Berlin, Germany; 473. p. 478–2011.
7. Feng AL, Boraey MA, Gwin MA, Finlay PR, Kuehl PJ, Vehring R. Mechanistic models facilitate efficient development of leucine containing microparticles for pulmonary drug delivery. Int J Pharm. 2011;409:156–63.
8. McCaughey G, McKevitt M, Elborn JS, Tunney MM. Antimicrobial activity of fosfomycin and tobramycin in combination against cystic fibrosis pathogens under aerobic and anaerobic conditions. J Cyst Fibros. 2012;11:163–72.
9. Cava F, Lam H, de Pedro MA, Waldor MK. Emerging knowledge of regulatory roles of d-amino acids in bacteria. Cell Mol Life Sci. 2011;68:817–31.
10. Stewart PS, Franklin MJ. Physiological heterogeneity in biofilms. Nat Rev Microbiol. 2008;6:199–210.
11. Ashish A, Shaw M, Winstanley C, Ledson MJ, Walshaw MJ. Increasing resistance of the Liverpool Epidemic Strain (LES) of Pseudomonas aeruginosa (Psa) to antibiotics in cystic fibrosis (CF)—A cause for concern? J Cyst Fibros. 2012;11:173–9.
12. Perez LRR, Barth AL. Biofilm production using distinct media and antimicrobial susceptibility profile of Pseudomonas aeruginosa. Braz J Infect Dis. 2011;15:301–4.
13. Ren CL, Konstan MW, Yegin A, Rasouliyan L, Trzaskoma B, Morgan WJ, *et al.* Multiple antibiotic-resistant Pseudomonas aeruginosa and lung function decline in patients with cystic fibrosis. J Cyst Fibros. 2012;11:293–9.
14. Tingpej P, Elkins M, Rose B, Hu H, Moriarty C, Manos J, *et al.* Clinical profile of adult cystic fibrosis patients with frequent epidemic clones of Pseudomonas aeruginosa. Respirology. 2010;15:923–9.
15. Kolodkin-Gal I, Romero D, Cao S, Clardy J, Kolter R, Losick R. D-amino acids trigger biofilm disassembly. Science. 2010;328:627–9.
16. Sanchez Z, Tani A, Kimbara K. Extensive reduction of cell viability and enhanced matrix production in pseudomonas aeruginosa PAO1 flow biofilms treated with a D-amino acid mixture. Appl Environ Microbiol. 2013;79:1396–9.
17. Stewart PS. A review of experimental measurements of effective diffusive permeabilities and effective diffusion coefficients in biofilms. Biotechnol Bioeng. 1998;59:261–72.
18. Vehring R. Pharmaceutical particle engineering via spray drying. Pharm Res. 2008;25:999–1022.
19. Javaheri E, Shemirani FM, Pichelin M, Katz IM, Caillibotte G, Vehring R, *et al.* Deposition modeling of hygroscopic saline aerosols in the human respiratory tract: comparison between air and helium-oxygen as carrier gases. J Aerosol Sci. 2013. doi:10.1016/j.jaerosci.2013.04.010.
20. Lange CF, Hancock REW, Samuel J, Finlay WH. In vitro aerosol delivery and regional airway surface liquid concentration of a liposomal cationic peptide. J Pharm Sci. 2001;90:1647–57.
21. Hasan MA, Lange CF. Estimating in vivo airway surface liquid concentration in trials of inhaled antibiotics. J Aerosol Med. 2007;20:282–93.
22. Weers JG, Tarara TE, Clark AR. Design of fine particles for pulmonary drug delivery. Expert Opin Drug Deliv. 2007;4:297–313.
23. Finlay WH, Stapleton KW, Zuberbuhler P. Fine particle fraction as a measure of mass depositing in the lung during inhalation of nearly isotonic nebulized aerosols. J Aerosol Sci. 1997;28:1301–9.
24. Stahlhofen W, Rudolf G, James AC. Intercomparison of experimental regional aerosol deposition data. J Aerosol Med. 1989;2:285–308.
25. Aquino RP, Prota L, Auriemma G, Santoro A, Mencherini T, Colombo G, *et al.* Dry powder inhalers of gentamicin and leucine: formulation parameters, aerosol performance and in vitro toxicity on CuFi1 cells. Int J Pharm. 2012;426:100–7.
26. Son YJ, Worth Longest P, Hindle M. Aerosolization characteristics of dry powder inhaler formulations for the excipient enhanced growth (EEG) application: effect of spray drying process conditions on aerosol performance. Int J Pharm. 2013;443:137–45.
27. Sou T, Kaminskas LM, Nguyen T-H, Carlberg R, McIntosh MP, Morton DAV. The effect of amino acid excipients on morphology and solid-state properties of multi-component spray-dried formulations for pulmonary delivery of biomacromolecules. Eur J Pharm Biopharm. 2013;83:234–43.
28. Hoe S, Matinkhoo S, Boraey MA, Ivey JW, Shamsaddini-Shahrbabak A, Finlay WH, *et al.* Substitution of L-Leucine with D-Leucine in spray-dried respirable powders for control of *Pseudomonas aeruginosa* infection. Chapel Hill: International Society for Aerosols in Medicine (ISAM); 2013.
29. Matinkhoo S, Hoe S, Boraey MA, Shamsaddini-Shahrbabak A, Finlay WH, and Vehring R: Spray drying D-amino acids to develop respirable dry powder for the treatment of Pseudomonas aeruginosa biofilms. American Association of Pharmaceutical Scientists (AAPS) Annual Meeting and Exposition: Chicago, IL,, 2012.
30. Adi S, Adi H, Tang P, Traini D, Chan HK, Young PM. Microparticle corrugation, adhesion and inhalation aerosol efficiency. Eur J Pharm Sci. 2008;35:12–8.
31. Weiler C, Egen M, Trunk M, Langguth P. Force control and powder dispersibility of spray dried particles for inhalation. J Pharm Sci. 2010;99:303–16.
32. Ogan Ó, Li J, Tajber L, Corrigan OI, Healy AM. Particle engineering of materials for oral inhalation by dry powder inhalers. I - Particles of sugar excipients (trehalose and raffinose) for protein delivery. Int J Pharm. 2011;405:23–35.
33. Shoyele SA, Cawthorne S. Particle engineering techniques for inhaled biopharmaceuticals. Adv Drug Deliv Rev. 2006;58:1009–29.

34. Hancock BC, Shamblin SL, Zografi G. Molecular mobility of amorphous pharmaceutical solids below their glass-transition temperatures. Pharm Res. 1995;12:799–806.
35. Zhou DL, Zhang GGZ, Law D, Grant DJW, Schmitt EA. Physical stability of amorphous pharmaceuticals: importance of configurational thermodynamic quantities and molecular mobility. J Pharm Sci. 2002;91:1863–72.
36. Dranca I, Bhattacharya S, Vyazovkin S, Suryanarayanan R. Implications of global and local mobility in amorphous sucrose and trehalose as determined by differential scanning calorimetry. Pharm Res. 2009;26:1064–72.
37. Ekdawi-Sever N, De Pablo JJ, Feick E, Von Meerwall E. Diffusion of sucrose and α, α-trehalose in aqueous solutions. J Phys Chem A. 2003;107:936–43.
38. Umecky T, Kuga T, Funazukuri T. Infinite dilution binary diffusion coefficients of several α-amino acids in water over a temperature range from (293.2 To 333.2) K with the taylor dispersion technique. J Chem Eng Data. 2006;51:1705–10.
39. Chan TL, Lippmann M. Experimental measurements and empirical modelling of the regional deposition of inhaled particles in humans. Am Ind Hyg Assoc J. 1980;41:399–409.
40. Heyder J. Gravitational deposition of aerosol particles within a system of randomly oriented tubes. J Aerosol Sci. 1975;6:133–7.
41. Heyder J, Gebhart J. Gravitational deposition of particles from laminar aerosol flow through inclined circular tubes. J Aerosol Sci. 1977;8:289–95.
42. Ingham DB. Diffusion of aerosols from a stream flowing through a cylindrical tube. J Aerosol Sci. 1975;6:125–32.
43. Vehring R. Red-excitation dispersive Raman spectroscopy is a suitable technique for solid-state analysis of respirable pharmaceutical powders. Appl Spectrosc. 2005;59:286–92.
44. Boraey MA, Hoe S, Sharif H, Miller DP, Lechuga-Ballesteros D, Vehirng R. Improvement of the dispersibility of spray-dried budesonide powders using leucine in an ethanol-water cosolvent system. Powder Technol. 2013;236:171–8.
45. Vehring R, Ivey JW, Williams L, Joshi V, Dwivedi S, and Lechuga-Ballesteros D: High-sensitivity analysis of crystallinity in respirable powders using low-frequency shift Raman spectrocopy. In: RN Dalby, PR Byron, J Peart, JD Suman, and PM Young, editors, Respiratory drug delivery Vol II. Davis Healthcare International Publishing; 2012. pp. 641–644.
46. Shamsaddini-Sharbabak A, Vehring R. The compression behavior of respirable powders at different relative humidity measured by a compressed bulk density tester for small sample masses. In: Dalby RN, Byron PR, Peart J, Suman JD, Young PM, editors. Respiratory drug delivery, vol. III. River Grove: Davis Healthcare International Publishing; 777. p. 780–2012.
47. Naini V, Byron PR, Phillips EM. Physicochemical stability of crystalline sugars and their spray-dried forms: dependence upon relative humidity and suitability for use in powder inhalers. Drug Dev Ind Pharm. 1998;24:895–909.
48. Raula J, Thielmann F, Naderi M, Lehto VP, Kauppinen EI. Investigations on particle surface characteristics vs. dispersion behaviour of l-leucine coated carrier-free inhalable powders. Int J Pharm. 2010;385:79–85.
49. Stapleton KW, Guentsch E, Hoskinson MK, Finlay WH. On the suitability of k-epsilon turbulence modelling for aerosol deposition in the mouth and throat:a comparison with experiment. J Aerosol Sci. 2000;31:739–49.
50. Chen XD, Sidhu H, Nelson M. Theoretical probing of the phenomenon of the formation of the outermost surface layer of a multicomponent particle, and the surface chemical composition after the rapid removal of water in spray drying. Chem Eng Sci. 2011;66:6375–84.
51. Roe KD, Labuza TP. Glass transition and crystallization of amorphous trehalose-sucrose mixtures. Int J Food Prop. 2005;8:559–74.
52. Ding SP, Fan J, Green JL, Lu Q, Sanchez E, Angell CA. Vitrification of trehalose by water loss from its crystalline dihydrate. J Therm Anal. 1996;47:1391–405.
53. Clark AR, Hollingworth AM. The relationship between powder inhaler resistance and peak inspiratory conditions in healthy volunteers – Implications for *in vitro* testing. J Aerosol Med. 1993;6:99–110.